Sensing Volume of Open-Ended Coaxial Probes for Dielectric Characterization of Breast Tissue at Microwave Frequencies

D. Popovic[1*], D. Hagl[2], C. Beasley[2],
M. Okoniewski[1], S. C. Hagness[2], and J. H. Booske[2]
(1) Department of Electrical and Computer Engineering, University of Calgary
2500 University Drive, Calgary N.W., Alberta, T2N 1N4
(2) Department of Electrical and Computer Engineering, University of Wisconsin
1415 Engineering Drive, Madison, WI 53706

I. Introduction

The University of Calgary (UC) and the University of Wisconsin-Madison (UW) are conducting comprehensive measurements of the dielectric properties of normal, benign, and malignant breast tissue to further facilitate the development of microwave technology for early breast cancer detection [1-4]. Measurements over the 0.1 to 20 GHz frequency range are taken using specially developed, small-diameter open-ended coaxial probes without flanges [5]. The end of the probe is placed in contact with the tissue sample and the complex input reflection coefficient is measured using a vector network analyzer (VNA) and numerically converted to sample permittivity.

To achieve accurate measurements, the tissue sample should be homogeneous within a volume large enough so that the measured reflection coefficient is identical to that of a sample filling the entire half-space. Thus, the question arises of the appropriate size of the tissue sample. Sensing volume guidelines have been previously investigated in terms of somewhat arbitrarily chosen constraints on the relative errors in the measured reflection coefficient of tissue-equivalent liquids [6]. In this paper we report sensing volume guidelines that have been developed by first choosing acceptable levels of error in the permittivity and then deriving the appropriate constraints on the errors in the measured reflection coefficient.

II. Methods

We investigate the sensing volume of the probe by tracking changes in the reflection coefficient as the fully immersed probe is placed at various distances from the edge or bottom of a beaker filled with a tissue-equivalent liquid. The extent of the sensing volume is identified as the smallest distance between the probe and boundary for which the reflection coefficient magnitude and phase errors remain below a defined error threshold.

The error threshold in the measured reflection coefficient is determined from an acceptable level of error in the measured permittivity, illustrated using the rational function model (RFM) [7] in conjunction with an innovative graphical technique based on Cole-Cole diagrams. Artificial incremental perturbations are introduced in the magnitude and phase of the reference reflection coefficient, which is then converted to complex permittivity across the 1 to 20 GHz range

0-7803-7846-6/03/$17.00 ©2003 IEEE

using the RFM. Fig. 1 shows a representative example of Cole-Cole diagrams for a 2.2 mm probe in water. Five ellipses centered at representative frequency points along the locus of complex permittivity values represent a $\pm 10\,\%$ variation in ε' and ε''. The ellipses enable us to graphically relate the acceptable level of error in permittivity to an upper bound on the error in the reflection coefficient. The error thresholds determined from this technique are summarized in Table I for 2.2- and 3.58-mm-diameter copper-Teflon probes.

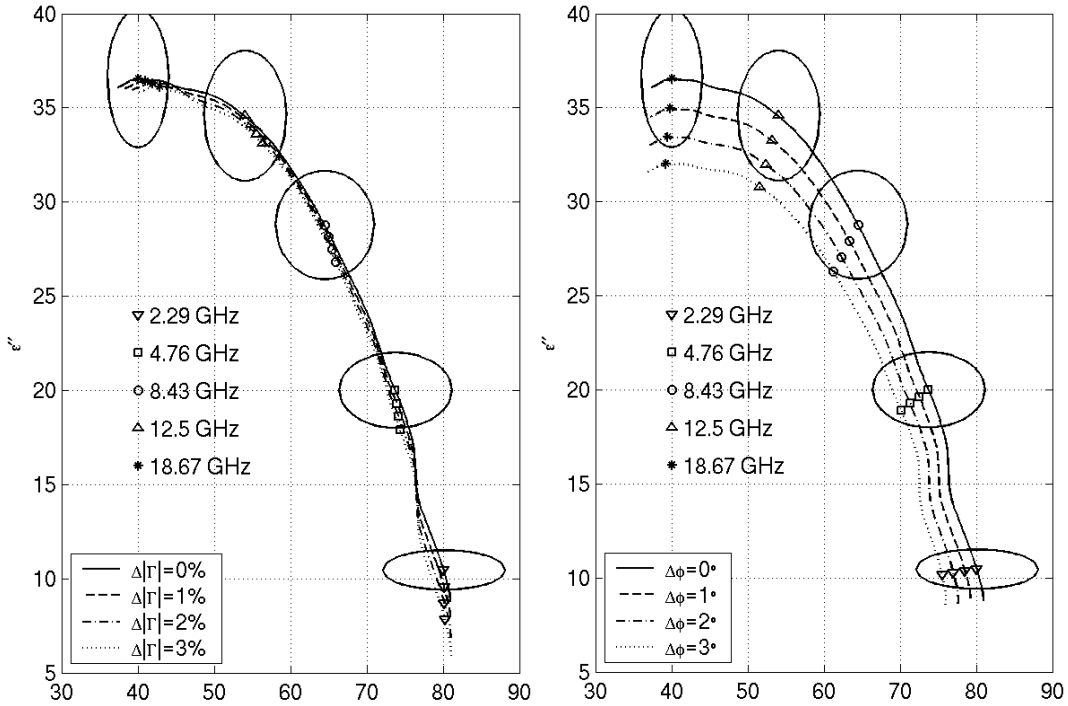

Fig. 1. Cole-Cole diagrams of complex permittivity as a function of frequency for the 2.2 mm probe in de-ionized water. The black solid curve represents the reference complex permittivity data. The various dotted curves represent the complex permittivity data resulting from a perturbation introduced in either the magnitude or phase of the reference reflection coefficient.

TABLE I
S_{11} Magnitude and Phase Error Thresholds that Limit the Error on Real and Imaginary Parts of the Permittivity to $\pm 10\,\%$

	S_{11} for Ethanol		S_{11} for Methanol		S_{11} for Water	
Probe Diameter	Mag. error ($\pm$ %)	Phase error ($\pm$ degrees)	Mag. error ($\pm$ %)	Phase error ($\pm$ degrees)	Mag. error ($\pm$ %)	Phase error ($\pm$ degrees)
2.2 mm	0.5-1.0	~0.5	0.5-1.0	1.0-1.5	~1.0	2.0-3.0
3.58 mm	1.0-1.5	~1.0	~1.5	2.0-2.5	~1.0	~1.0

We note that the probe is fully immersed into the liquids to remove all uncertainties involving the positioning of the probes. To determine what impact, if any, this configuration may have on the determination of the sensing volume, we have analyzed the distribution of the fringing fields beneath the probe using FDTD simulations. Two representative cases are shown in Fig. 2 and Fig. 3. Considering the location of the -30 dB contours in the half-space beneath each probe, we observe less than a 0.1-mm difference in the position of the contours in

the axial direction. In the radial direction, there is only a 0.2-mm difference for the larger probe in ethanol at 2 GHz (Fig. 2), and a 0.1-mm difference for the smaller probe in water at 18 GHz (Fig. 3). These differences are insignificant for the purposes of quantifying the sensing volume.

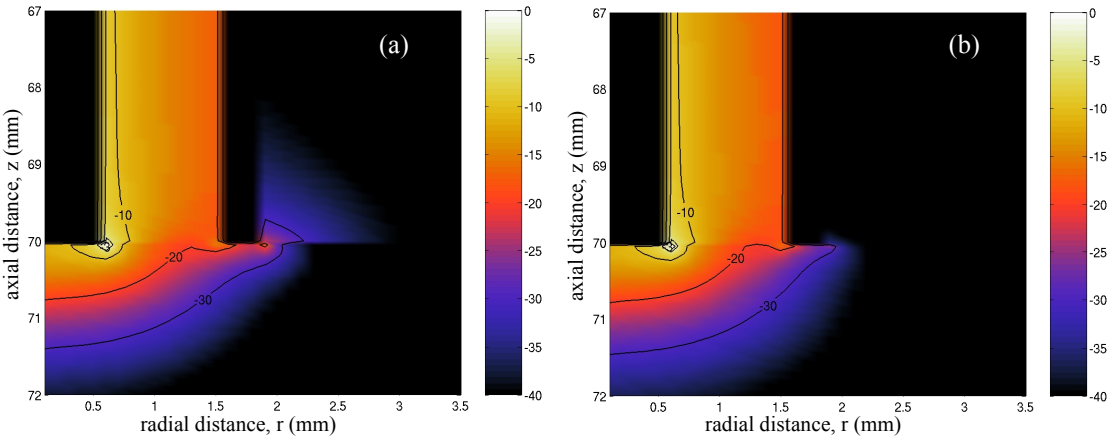

Fig. 2. Contour plots of the FDTD-computed electric field intensity (dB scale) in a cross-sectional cut through the 3.58-mm-diameter probe in ethanol at 2 GHz. (a) The probe is placed in contact with the surface of the LUT. (b) The probe is immersed at a depth of 10 mm in the LUT. The left boundary of each graph represents the center axis of the probe.

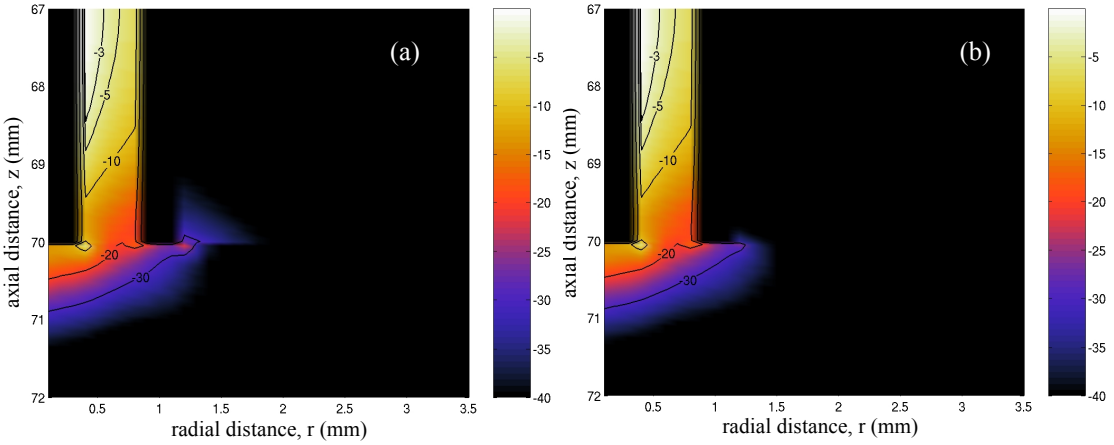

Fig. 3. Contour plots of the FDTD-computed electric field intensity (dB scale) in a cross-sectional cut through the 2.2-mm-diameter probe in water at 18 GHz. (a) The probe is placed in contact with the surface of the LUT. (b) The probe is immersed at a depth of 10 mm in the LUT.

III. Results

Relative errors in the magnitude and phase of the reflection coefficient at various distances from the beaker walls are calculated from the measured data. These results are used to identify the minimum distance in the axial and radial directions for which the errors are below the thresholds specified in Table I for each liquid under test (LUT) and probe. Estimates for the sensing volume of the 2.2 mm and 3.58 mm probes are summarized in Table II. According to the data of Table II, the sensing volume is greater for the larger-diameter probe and a function of the LUT.

TABLE II
Sensing Depth and Radial Sensing Dimension as a Function of LUT and Probe Aperture Size Determined Through Experiment and Simulation

Probe diameter	Sensing dimension	Ethanol	Methanol	Water
2.2 mm	axial	0.75-1.0 mm	1.0-1.5 mm	~1.5 mm
	radial (simulated)	<0.5 mm	0.5-1.0 mm	~1.25 mm
3.58 mm	axial	1.25-1.5 mm	~2.25 mm	~2.5-3.0 mm
	radial (simulated)	<0.5 mm	~1.0 mm	3.5-3.75 mm

Excellent agreement is obtained between experimental and simulation results for the sensing depth. In the case of radial sensing dimension, the experiments showed that the influence of the beaker wall is minimal, even when the probe is in direct contact with the side of the beaker. For all liquids and all probes, there is no required distance of separation between the outer conductor of the probe and the non-concentric radial boundary. This suggests that accurate measurements can be made with the probe located at the edge of a specimen or region of homogeneous tissue as long as the radius of curvature of the boundary is much larger than that of the probe's outer conductor. On the other hand, the probe and beaker radii are concentric in the simulation model, showing much stronger influence of the radial boundary on the simulated reflection coefficient, as expected.

IV. Conclusions

For frequencies between 1 GHz and 20 GHz, the thickness of the breast tissue specimen (or extent of homogeneity in the case of a larger specimen) should be greater than 3.0 mm for a 3.58 mm probe and greater than 1.5 mm for a 2.2 mm probe. The full transverse extent of the specimen (or homogeneous region of tissue) should be at least 1.1 cm for the 3.58 mm probe and at least 5 mm for the 2.2 mm probe in order to bound the permittivity error to approximately 10%. For much larger specimens, accurate measurements may be achieved regardless of how close the outer diameter of the probe is to the margin.

References

[1] S. C. Hagness, A. Taflove, and J. E. Bridges, "Two-dimensional FDTD analysis of a pulsed microwave confocal system for breast cancer detection: Fixed-focus and antenna-array sensors," *IEEE Trans. Biomed. Eng.*, vol. 45, pp. 1470-1479, Dec. 1998.

[2] X. Li and S. C. Hagness, "A confocal microwave imaging algorithm for breast cancer detection," *IEEE Microwave Wireless Components Lett.*, vol. 11, pp. 130-132, Mar. 2001.

[3] E. Bond, X. Li, S. C. Hagness, and B. D. Van Veen, "Microwave imaging via space-time beamforming for early detection of breast cancer," *IEEE Trans. Antennas Propagat.*, in press.

[4] E.C. Fear and M. A. Stuchly, "Microwave detection of breast cancer", *IEEE Trans. Microwave Theory Tech.*, vol. 48, no. 11, pp. 1854-1863, Nov. 2000.

[5] D. Popovic and M. Okoniewski, "Precision open-ended coaxial probe for dielectric spectroscopy of breast tissue", in *IEEE Antennas Propagat. Soc. Int. Symp.*, San Antonio, TX, June 2002, vol. 1, pp. 815-818

[6] D. Popovic, M. Okoniewski, D. Hagl, J. H. Booske, and S. C. Hagness, "Volume sensing properties of open-ended coaxial probes for dielectric spectroscopy of breast tissue", in *IEEE Antennas Propagat. Soc. Int. Symp.*, Boston, MA, July 2001, vol. 1, pp. 254-257

[7] J.M. Anderson, C.L. Sibbald, and S.S. Stuchly, "Dielectric measurements using a rational function model", *IEEE Trans. Microwave Theory Tech.*, vol.42, pp.199-204, 1994.